Recent burning of boreal forests exceeds fire regime limits of the past 10,000 years

Ryan Kelly[a], Melissa L. Chipman[b], Philip E. Higuera[c], Ivanka Stefanova[d], Linda B. Brubaker[e], and Feng Sheng Hu[a,b,1]

[a]Department of Plant Biology and [b]Program in Ecology, Evolution, and Conservation Biology, University of Illinois, Urbana, IL 61801; [c]Department of Forest, Rangeland, and Fire Sciences, University of Idaho, Moscow, ID 83844-1133; [d]Limnological Research Center, University of Minnesota, Minneapolis, MN 55455; and [e]School of Environmental and Forest Sciences, University of Washington, Seattle, WA 98195

Edited by Thompson Webb, Brown University, Providence, RI, and accepted by the Editorial Board June 19, 2013 (received for review March 15, 2013)

Wildfire activity in boreal forests is anticipated to increase dramatically, with far-reaching ecological and socioeconomic consequences. Paleorecords are indispensible for elucidating boreal fire regime dynamics under changing climate, because fire return intervals and successional cycles in these ecosystems occur over decadal to centennial timescales. We present charcoal records from 14 lakes in the Yukon Flats of interior Alaska, one of the most flammable ecoregions of the boreal forest biome, to infer causes and consequences of fire regime change over the past 10,000 y. Strong correspondence between charcoal-inferred and observational fire records shows the fidelity of sedimentary charcoal records as archives of past fire regimes. Fire frequency and area burned increased ∼6,000–3,000 y ago, probably as a result of elevated landscape flammability associated with increased *Picea mariana* in the regional vegetation. During the Medieval Climate Anomaly (MCA; ∼1,000–500 cal B.P.), the period most similar to recent decades, warm and dry climatic conditions resulted in peak biomass burning, but severe fires favored less-flammable deciduous vegetation, such that fire frequency remained relatively stationary. These results suggest that boreal forests can sustain high-severity fire regimes for centuries under warm and dry conditions, with vegetation feedbacks modulating climate–fire linkages. The apparent limit to MCA burning has been surpassed by the regional fire regime of recent decades, which is characterized by exceptionally high fire frequency and biomass burning. This extreme combination suggests a transition to a unique regime of unprecedented fire activity. However, vegetation dynamics similar to feedbacks that occurred during the MCA may stabilize the fire regime, despite additional warming.

paleoecology | Holocene | Arctic | climate change | climate–fire–vegetation interactions

The vast boreal forest biome is a crucial component of the Earth system, representing almost 10% of the land surface and >30% of terrestrial carbon stocks (1). Boreal ecosystems have undergone pronounced changes in recent decades in response to climatic warming (2), including increased forest burning, permafrost melting, and wetland drying. Changes in fire activity have gained special attention because of the potential for dramatic effects at multiple scales. Natural, stand-replacing wildfires are the principal disturbance in these ecosystems, and they release copious amounts of carbon directly through combustion of biomass and soil organic matter (3). Additionally, postfire succession occurs over many decades, with interacting effects on biogeochemical cycles (4), energy balance (5), and hydrology (6), all of which can produce climate feedbacks. Understanding these dynamics is essential to projecting future environmental change from local to global scales.

The present understanding of boreal fire regimes is largely based on several decades of observational studies. Interannual variability in fire activity is related to seasonal climate (7, 8), and recent extreme fire years occurred under exceptionally warm and/or dry conditions (9). These relationships form the basis of various predictive models, which almost ubiquitously suggest increased frequency, size, and/or severity of burns in coming decades as a result of future warming (summarized in ref. 10). However, such projections often do not consider potentially important climate–fire–vegetation interactions. In particular, climate-driven increases in boreal forest burning may lead to the dominance of early successional deciduous vegetation and thereby produce a negative feedback to additional burning (9, 11). Because fire return intervals and successional cycles in the boreal forest occur over decadal to centennial timescales, the observational fire records of the past several decades are of limited use for understanding fire regime dynamics in these ecosystems.

Paleoecological analysis is indispensable for elucidating the causes and consequences of ecosystem change over a broad range of environmental conditions and temporal scales. Here, we present results of charcoal analysis on sediment cores from 14 lakes in the Yukon Flats (YF) ecoregion of interior Alaska. We take advantage of the exceptionally high spatial density of our charcoal records to quantitatively evaluate the fidelity of sedimentary charcoal as a proxy indicator of past fire regimes. We then discuss variations in fire frequency, biomass burning, and fire severity in relation to climate and vegetation change at centennial to millennial timescales. These data allow us to put fire regime dynamics of the past several decades in the context of natural variability of past millennia and infer the role of climate–fire–vegetation interactions in boreal forest burning. We chose the YF ecoregion for this study because its recent fire frequencies are among the highest in the North American boreal forests (12, 13), corresponding to warm and dry summers in the region. Thus, this ecoregion is well-suited to serve as an upper bound on past and current burning in the boreal forest biome.

Results and Discussion

Validation and Interpretation of Charcoal Records. Charcoal analysis of lake sediments is widely used to quantify fire frequency and the relative amount of biomass burning through time (14, 15). Although this approach is generally supported theoretically (16) and empirically (17, 18), data remain limited for direct verification. Our study is particularly well-suited to address this limitation, as our sampling design provides unusually high spatiotemporal resolution (14 sites within an ∼1,000-km^2 region and median near-surface resolution of ∼5 y/sample). In addition, widespread recent burning in our study area ensures that ample fire data are available for comparison with the charcoal record, even in the short span of observational records [1950 CE (Common Era) to present]. We capitalize on these characteristics to

Author contributions: R.K., P.E.H., L.B.B., and F.S.H. designed research; R.K., M.L.C., P.E.H., I.S., and F.S.H. performed research; R.K. analyzed data; and R.K. and F.S.H. wrote the paper.

The authors declare no conflict of interest.

This article is a PNAS Direct Submission. T.W. is a guest editor invited by the Editorial Board.

Data deposition: The data reported in the paper have been deposited in the National Oceanic and Atmospheric Administration (NOAA) Paleoclimate Database, www.ncdc.noaa.gov/paleo/data.html.

[1]To whom correspondence should be addressed. E-mail: fshu@life.illinois.edu.

This article contains supporting information online at www.pnas.org/lookup/suppl/doi:10.1073/pnas.1305069110/-/DCSupplemental.

validate sedimentary charcoal records as archives of past fire regime change.

A number of recent studies have inferred total biomass burning from multi-site records of charcoal accumulation rate (CHAR) in sediments (15). To evaluate this approach, we compared a decadal composite of our 14 CHAR records with observations of area burned at a range of spatial scales defined by specified radii around each study lake (Fig. 1). The composite CHAR record exhibits a broad maximum centered on 1990 CE and secondary peaks in 1966 and 2005 CE (Fig. 2*A*). These features are generally visible in the observed record of area burned. The two time series are significantly correlated ($r > 0.75$, $P < 0.01$) at scales of up to 20 km, with maximum agreement at the 5-km scale ($r = 0.91$, $P < 0.001$). The correlation becomes nonsignificant at >20-km scales (Fig. 2*B*). These results agree with charcoal dispersal simulations (16) and empirical findings (17), which indicate optimal correlation between sampled CHAR and area burned at intermediate (10^0–10^1 km) distance from individual sampling sites.

Distinct peaks in sediment charcoal time series are thought to record individual fire events near the sampling site (14), allowing the calculation of local fire frequency (FF). In our composite charcoal record, mean FF across all sites for the period 1950–2008 CE is 19.8 fires/ky, which relates well to FF estimated from the observed proportion of the landscape burned from 1950 to 2008 CE. Maximum agreement is at the 1-km scale, which yields an observation-based FF estimate of 18.5 fires/ky (7% error). This agreement is relatively robust (<20% error) at scales of up to 10 km (Fig. 2*C*), but it deteriorates sharply (>90% error) at scales of 50–100 km, for which the observed proportion of the landscape burned is much less than around the study sites. Compared with CHAR, the fidelity of reconstructed FF to observations declines more steeply with increasing spatial scale (Fig. 2 *B* and *C*).

Although charcoal peaks and average CHAR in individual records are often considered to represent local vs. regional signals, respectively, our results suggest that sampling a network of sites lessens this distinction. In particular, both our CHAR and FF composite records reliably capture fire activity within a contiguous area of at least 2,000 km^2 (equivalent to a 10-km radius). The good correspondence between our charcoal-inferred fire history and observational fire records provides some of the strongest empirical evidence to date in support of the prevailing assumptions in interpreting sediment charcoal data. These results lend credence to our Holocene reconstructions for the YF and also add support to a growing body of literature analyzing composite CHAR records to infer broad-scale patterns of past fire regime variability (15, 18–20). Furthermore, to the extent that validation of our charcoal records may have been facilitated by multiple sites and high-resolution sampling as described above, these results should motivate similar designs where detailed fire history reconstructions are required. We acknowledge, however, that sediment charcoal analysis is best suited for reconstructing high-severity fires in landscapes with relatively low topographic complexity; lower charcoal production or more complex terrain would confound the signal of fire and increase variability among sites (17, 21).

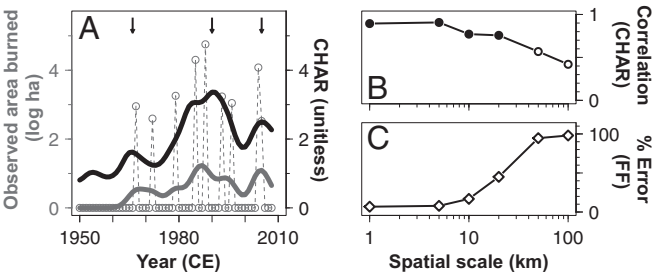

Fig. 2. Validation of sediment charcoal data with observed fire history since 1950 CE. (*A*) Comparison of decadal composite CHAR and observed area burned at the optimal spatial scale for comparison (5 km) (Fig. 1). Annual area burned observations (dashed gray) were decadally smoothed (solid gray) and compared with the CHAR record (black). Arrows indicate maxima noted in the text. (*B*) Spatial dependence of CHAR validation results; statistically significant ($P < 0.01$) and nonsignificant ($P > 0.05$) correlations are indicated by solid and open circles, respectively. (*C*) Spatial dependence of FF validation results, indicating the percent error between mean FF estimated from charcoal peaks vs. observed proportion of the landscape burned since 1950 CE.

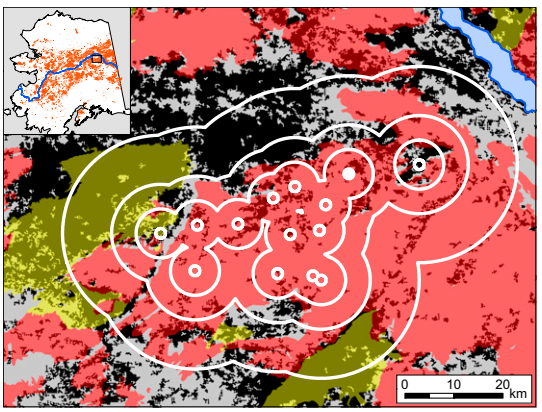

Fig. 1. The study area highlighting observed fire history (1950–2010 CE), land cover, and spatial scales discussed in the text. Land cover is based on satellite imagery collected in 2005 CE (47) and reclassified as coniferous (black; i.e., *Picea*) or nonconiferous (gray). Observed fire perimeters represent burns that occurred before (red) and after (yellow) collection of the land cover data in 2005 CE. Spatial domains defined by radii of 1, 5, 10, and 20 km around each study site (white circles) were used when quantifying observed fire history as validation data (50- and 100-km spatial scales discussed in text are not shown). Pollen data were collected from Screaming Lynx Lake (filled circle). *Inset* shows the location of the study area in Alaska (black box) and the observed fire perimeters statewide (orange). The Yukon River (blue) is shown for spatial reference.

Centennial to Millennial Fire Regime Variability of the Past 10,000 y. Our charcoal record reveals distinct patterns of fire regime change in relation to climatic and vegetational shifts over the past 10,000 y. At millennial timescales, composite CHAR is around 0.5 (dimensionless because of standardization) (*Methods*) and relatively constant during the early Holocene (Fig. 3*A*). It begins increasing at *ca.* 6,000 calibrated years (cal) B.P. and continues to rise, with some oscillations, to a maximum of 2.0 around 800 cal B.P. Millennial FF is more variable but also relatively low before 6,000 cal B.P. (mean = 5.6 fires/ky) and higher in the late Holocene, especially after 3,000 cal B.P. (mean = 8.6 fires/ky) (Fig. 3*B*). The increases in CHAR and FF coincide with the steady increase of *Picea mariana* (black spruce) pollen from trace levels (<3%) before 6,000 cal B.P. to modern abundance (~15%) by ~3,000 cal B.P. (Fig. 3*D*). These inferred changes in fire regime and vegetation are based on the subset of our records that span the early and middle Holocene, and thus benefit least from the spatial replication of our study design (Fig. 3*C*). Nevertheless, the results are consistent with several prior studies in Alaska documenting increased fire activity in association with the mid-Holocene expansion of *P. mariana* (22, 23). *P. mariana* is the most flammable species in Alaskan boreal forests today, with adaptations to both promote and persist through fire (e.g., high resin content and semi-serotinous cones) (24). The expansion of this species and associated increase in landscape-scale flammability probably drove the late Holocene rise in FF and overall rates of biomass burning. Furthermore, the mid-Holocene increase in summer temperature in the region (25) may have played a role in promoting forest burning.

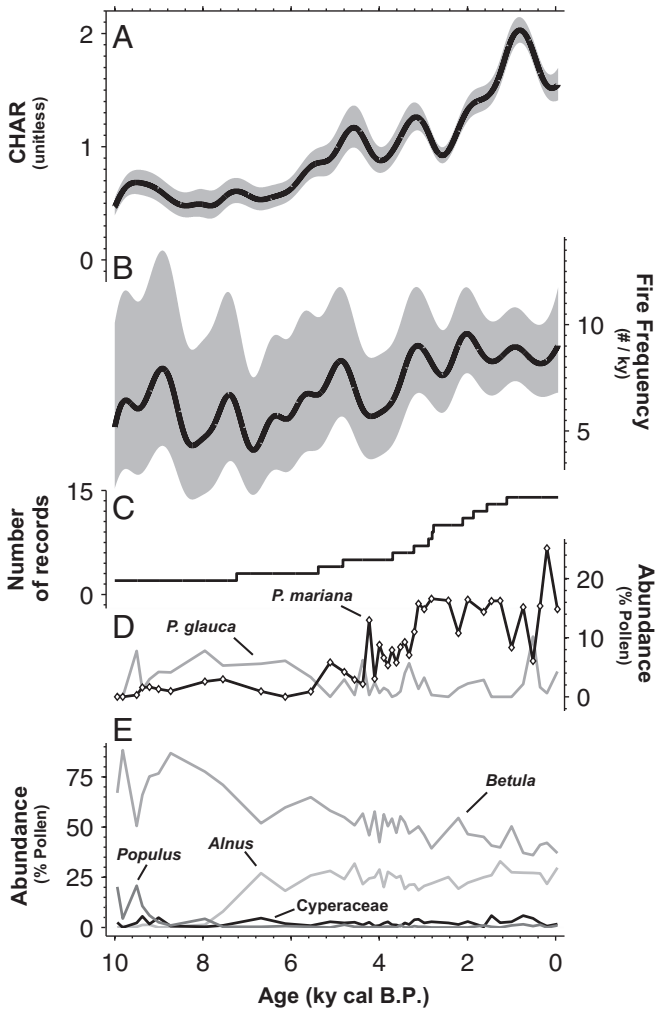

Fig. 3. Proxy records of ecosystem change, highlighting millennial patterns of the past 10,000 y. Millennial composite records of (*A*) CHAR and (*B*) FF from sediment charcoal analysis (with 90% confidence intervals). (*C*) Number of records contributing to composite charcoal records. Pollen abundance of (*D*) key conifer species *P. mariana* and *P. glauca* and (*E*) other major taxa at Screaming Lynx Lake (Fig. 1). Diamond symbols on the *P. mariana* curve indicate sampling resolution for all pollen data.

Over the past 3,000 y, the regional vegetation has remained broadly similar to modern boreal forests (Fig. 3 *D* and *E*), although high-resolution pollen analysis suggests climatically driven shifts in species composition during this period (26). Inferences of biomass burning from CHAR display centennial-scale patterns (Fig. 4*A*) coincident with several known climatic fluctuations. In particular, the broad CHAR peak at *ca.* 1,000–500 cal B.P. suggests increased biomass burning during the Medieval Climate Anomaly (MCA). The MCA is known to have been a warm and drought-prone period in many regions globally (27). In Alaska, lake sediment analyses suggest near-modern temperature during the MCA (28, 29) accompanied by relatively arid conditions (29, 30), perhaps analogous to the recent trend of diminishing water availability driven by increased evapotranspiration because of warming (31). After the MCA, composite CHAR declines to a brief minimum (1.0) during the Little Ice Age (LIA), which was characterized by cooler (25, 28) and wetter (29) conditions in the region. The subsequent sharp rise in CHAR to values similar to the MCA peak corresponds to marked warming and increased forest burning in Alaska during the past few decades (32). Transient vegetation shifts inferred from pollen (Fig. 3 *D* and *E*) may have influenced the fire regime as well (see below). Nonetheless, over the last 3,000 y, climatic variation seems to have exerted a dominant control over biomass burning in the YF at centennial timescales. This interpretation is consistent with the observational record of the past 60 y, which shows increased area burned during warmer and/or drier years in boreal forest ecosystems (7, 8).

Compared with CHAR, composite FF exhibits less pronounced variability corresponding to the MCA and LIA. At centennial scales, FF varies markedly around a relatively stationary mean of ~9 fires/ky throughout most of the last 3,000 y (Fig. 4*B*), with low correlation to CHAR ($r = 0.33$, $P = 0.02$). This pattern stands in contrast to the general similarity in millennial-scale CHAR and FF trends throughout much of the past 10,000 y. Changes in the degree of coupling between biomass burning and FF may themselves represent fire regime properties. Indeed, a recent study (18) considered variability in the CHAR:FF ratio as a measure of fire size, an interpretation that is rational given the demonstrable relationship between CHAR and area burned in recent decades (see above). However, over broad spatiotemporal scales, the CHAR:FF ratio should remain approximately constant if CHAR reflects area burned only. This is because both area burned and FF are directly related to fire

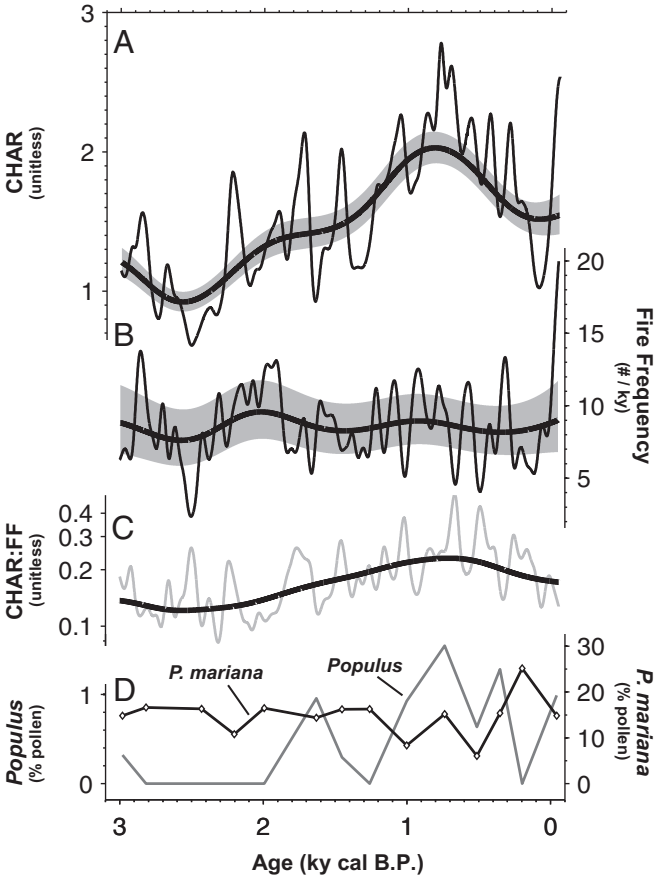

Fig. 4. Ecosystem change over the past 3,000 y. The sources of these pollen and charcoal data are the same as in Fig. 3, but here, we highlight centennial variability since the establishment of modern boreal forests in the study region ~3,000 cal B.P. Centennial (thin lines) and millennial (thick lines; with 90% confidence intervals) composite records of (*A*) CHAR and (*B*) FF from sediment charcoal analysis. (*C*) Ratio of CHAR to FF representing fire severity; centennial patterns are illustrated (gray line), but only millennial trends (black line) are interpreted (*Results and Discussion*). (*D*) Pollen abundance of dominant late successional *P. mariana* and key postfire recruit *Populus* at Screaming Lynx Lake (Fig. 1), with diamond symbols indicating sampling resolution of both taxa.

ECOLOGY

probability at any given point in space and time, and are thus statistically identical (33). We reason that variation in the CHAR:FF ratio reflects changes in the amount of biomass consumed at a given FF, and based on this rationale, we consider this ratio as a proxy indicator of fire severity. We emphasize that this interpretation of the CHAR:FF ratio implicitly assumes that CHAR and FF represent fire on the same spatial scale. Our validation results support this assumption in the case of the YF composite records, but caution should be exerted when using the CHAR:FF ratio as a fire severity index in studies with lower spatial resolution. Furthermore, because the CHAR:FF ratio combines uncertainty in both CHAR and FF, we consider the ratio a semiquantitative proxy indicator, for which field validation remains to be done because of the paucity of observational fire severity data. We therefore restrict our interpretations to the most pronounced broad-scale patterns.

Overall, the record of the CHAR:FF ratio at our study sites varies similarly to CHAR during the past 3,000 y (Fig. 4*C*), suggesting that the impacts of centennial climate change on biomass burning were mainly driven by variations in fire severity. This CHAR:FF record reveals that fire severity increased from 3,000 cal B.P. to a maximum around 800 cal B.P. during the MCA and declined thereafter to present. Thus, warm and dry climatic conditions during the MCA seem to have resulted in peak severity but little change in FF. One plausible explanation is that the high-severity fires during this period promoted an unusual abundance of low-flammability deciduous species on the YF landscape. Deciduous recruitment is common during early succession after boreal fires, and the postfire success and persistence of deciduous species are partly dictated by burn severity (34, 35). High-severity fires characterized by extensive combustion of the soil organic layer favor deciduous regeneration, which may slow recovery to conifer dominance and in some cases disrupt an otherwise resilient cycle of *P. mariana* self-replacement (36). During the MCA, these mechanisms could have reduced the relative abundance and connectivity of flammable *P. mariana* vegetation, decreasing the probability of fire at the landscape scale and exerting a negative feedback to FF. Our pollen record (Fig. 4*D*) supports this interpretation. From 1,000 to 500 cal B.P., when fire severity was maximal, *P. mariana* dipped to its lowest abundance of the past 3,000 y. Concurrently, the percentages of *Populus tremuloides*-type pollen reached their highest values since the early Holocene, a striking signal given the notorious underrepresentation of *Populus* pollen in sediment records. *P. tremuloides* is a major component of postfire deciduous vegetation in Alaska today. Thus, severe fires during the MCA seem to have favored deciduous recruitment in the YF region, effectively limiting FF despite climate conditions highly conducive to burning.

Pushing the Limits: Recent Fire Regime Dynamics and Implications for Future Change. Although the timing and magnitude of the MCA were spatially heterogeneous, temperatures during the period approached 20th century values across much of the Northern Hemisphere, and many areas experienced exceptional hydroclimatic variability (27). Paleorecords of the period thus offer an opportunity to assess the ecosystem impacts of ongoing and future climate change (37). Here, we juxtapose recent burning in the YF with fire regime dynamics of the MCA and discuss implications for future change.

Our data reveal that FF is higher in recent decades than at any other time since the establishment of modern boreal forests 3,000 y ago. This charcoal-based estimate is supported by observational fire data. Concurrently, biomass burning inferred from CHAR has risen sharply to a level on par with the MCA maximum. Thus, the present fire regime seems to have surpassed the vegetation-induced limit that constrained burning during the MCA. Two factors may have contributed to this recent fire regime change. First, growing evidence suggests that climatic conditions of recent decades exceeded the range of variability during the MCA (27), which has probably favored forest burning (38). Second, the LIA fire regime was characterized by comparatively low fire frequency and severity, and exceptionally low biomass burning (Fig. 4 *A*–*C*). This combination should have led to high abundance and connectivity of flammable coniferous vegetation, effectively priming the landscape for widespread burning when suitable climatic conditions arose during recent decades. This hypothesis is supported by the maximum abundance of *P. mariana* pollen during the LIA (Fig. 3*D*), although the coarse temporal resolution of our pollen record prevents a rigorous evaluation. Simulation modeling has also suggested that recent increases in forest burning in interior Alaska resulted, in part, from prior fuel accumulation because of reduced past burning (38).

The extreme combination of exceptionally high CHAR and FF in recent decades may signal a transition to a novel regime of unprecedented fire activity in the YF. This possibility is in accord with numerous model simulations predicting dramatic acceleration of boreal forest burning under climate warming scenarios of the 21st century (10). Projections for Alaska and Western Canada, for instance, include a fivefold increase in annual area burned (8). Such prognoses join a burgeoning list of exceptional changes in high-latitude ecosystems in response to ongoing climate warming (39). These changes include extensive permafrost thaw (40) and associated thermokarst formation (41), treeline (42) and shrub (43) expansion, increased tundra burning (44), and loss of Arctic sea ice (45). Given that fire is the dominant process controlling carbon cycling in boreal ecosystems (4) and that increased biomass burning is already linked to carbon losses in Alaska (46), the unprecedented fire regime shift suggested by our data is potentially an important driver shaping the trajectory of high-latitude ecosystem changes.

Our study also suggests an alternative future trajectory by highlighting the importance of fire–vegetation interactions in the long-term dynamics of boreal fire regimes. By analogy to our MCA record from the YF, severe and extensive forest burning on the modern landscape could initiate vegetation feedbacks to dampen additional fire regime change. Late-season burning has increased over recent decades among YF fires (Fig. S1), mirroring a regional trend linked to increasing severity (46). Similar to climate–fire–vegetation interactions during the MCA, this trend may lead to increased deciduous cover on the YF landscape and a return to a fire regime more typical of the past 3,000 y. In support of this prediction, 62.3% of our study area (20-km radius around each site) was covered by non-spruce vegetation (deciduous and mixed forest classes as well as several early successional types) in 2005 CE (47). Spatially, this vegetation distribution corresponds well to fire locations before 2005 CE, and subsequent burn perimeters encompass 34.9% of the spruce cover that remained at that time (Fig. 1). Thus, forest burning in recent decades has already converted much of the YF landscape to a fragmented mosaic of lower-flammability vegetation. Satellite analysis (9) and plot-level measurements (48) also suggest that boreal ecosystems in Alaska are transitioning to a more deciduous-rich state as a result of recent severe fires, and model simulations indicate that this feedback will dampen the direct impact of warming on the future fire regime of boreal forests (11, 38). If this prediction is realized, recent burning may mark the initiation of an active but stable fire regime similar to the fire regime of the MCA. In this scenario, unprecedented fire activity of the past several decades will prove to be a transient anomaly, probably facilitated by rapid recent climate change and LIA fuel accumulation but unsustainable in the longer term.

Our results suggest that the fire regime of the YF ecoregion is presently beyond a limit defined by fire–vegetation feedbacks that constrained fire activity in the past several millennia. Recent burning in this region is among the most extensive of all North American boreal forests (12, 13), and it is likely that much of the biome has yet to reach such a vegetation-limited state. Fire activity is expected to increase in response to climate change in boreal forests worldwide (49), and as a result, deciduous cover may become a common feature of the biome (50). The modern YF landscape may therefore provide a future analog for other regions as they become increasingly fire-prone in a warming climate.

Ecosystem changes of the coming decades in this region—either to an MCA-like regime of prolonged high-severity burning or a new state unparalleled in Holocene history—could serve as a harbinger of biome-wide changes to come. Our fire reconstructions from the YF reveal that the boreal forest can sustain a high-severity fire regime for centuries under warm and arid conditions, but they also suggest that vegetation feedbacks attenuated the climate–fire relationship over these timescales in the past. Such dynamics have potentially dramatic ecological impacts (9, 48) that could interact with or override the direct effects of shifting climate and fire regime. Estimating the long-term trajectory of boreal forest ecosystems thus requires understanding if and how these feedbacks will progress under scenarios of future change.

Methods

Sites and Sediment Cores. Our sites are located near the southern boundary of the YF ecoregion in the foothills of the White Mountains. The area experiences a highly continental climate, with average daily temperatures ranging from −29 °C in January to 11 °C in July, and average annual precipitation of only 170 mm (51). Boreal forests typical of interior Alaska dominate the regional landscape, with extensive lowlands and permafrost soils providing abundant habitat for *P. mariana*, although *P. glauca* dominates on well-drained sites (51). The region has the lowest fire return interval in Alaska at present (12), and the modern landscape supports a mosaic of plant communities in various stages of postfire succession.

We selected small, deep lakes with minimal stream input. At 3 of 14 lakes, we used a Livingstone-type corer to collect two parallel overlapping sediment cores through the entire sediment thickness and a polycarbonate piston corer to retrieve the sediment–water interface. At the remaining 11 lakes, we used a polycarbonate piston corer to collect a sediment core of up to ∼1.2 m in length that spanned the intact sediment–water interface. We sliced the upper 10–20 cm of each surface core in the field at 0.5-cm increments, and the remainder was split lengthwise and sliced at 0.25-cm resolution in the laboratory. Magnetic susceptibility measurements on subsamples from each slice were used to corroborate visual correlation of cores with multiple drives.

Age Models. We developed chronologies from 139 ^{210}Pb and 75 ^{14}C ages (Table S1). For the upper 10–20 cm of each core, we analyzed bulk sediments at 1- to 2-cm intervals for ^{210}Pb activity (52) using an OctêtePlus Alpha Spectrometer at the University of Illinois. Sample age was estimated using the constant rate of supply model described in ref. 52. Age–depth models for sediments older than 150 y were based on accelerator MS ^{14}C ages of terrestrial macrofossils. Terrestrial macrofossils were treated with an acid–base–acid procedure (53) and submitted to Lawrence Livermore National Laboratory for radiocarbon measurements. Radiocarbon ages were calibrated using CALIB 6.1.1 (54) with the IntCal09 dataset.

Most of our cores consisted primarily of two discrete sediment types: dark-brown to black gyttja and fine gray silt. Typically, the latter was found in narrow bands (∼1–20 mm), but several cores had large silt layers tens of centimeters thick. We assumed that this material was deposited in rapid erosional or turbidite events, which was supported by discrete banding, low concentration of organic material and charcoal (determined visually under magnification), and high magnetic susceptibility. Thus, to avoid error from applying an age model based on smoothly varying sedimentation rate, we used a methodology that accounts for the dual sediment types, similar to the approach used in ref. 55 but modified to allow nonlinear variation in the sedimentation rate of the nonsilt sediments (*SI Methods*).

Charcoal and Pollen Analyses. We extracted macroscopic charcoal particles (>180 μm) from each core using standard methods. Charcoal particle concentrations (pieces per cm^3) were multiplied by sediment accumulation rate (cm per year; determined from age–depth models) to obtain CHAR (pieces per cm^2 per year).

Pollen identification was performed on one of our sediment cores (Screaming Lynx Lake) (Fig. 1) at varying intervals (median = 187 y). Sample preparation followed standard protocols for lake sediments (56), and pollen grains were counted at 40–100× magnification. Pollen data were expressed as a percentage of total pollen grains from terrestrial plants. *Populus* pollen was identified as the *P. tremuloides* type, which may include several species. However, the type is distinct from *P. balsamifera*, the only *Populus* species other than *P. tremuloides* that occurs in the study region at present. Thus, we assume that our *Populus* pollen came from *P. tremuloides*.

Estimating Frequency of Fire Events. To identify local fire events, we performed charcoal peak analysis on each of our records using the method in ref. 23 (see *SI Methods* for details). To derive a composite record representing regional average FF, we first pooled the identified fire events from all records and then computed kernel-weighted event counts over the period spanned by two or more records (10,330 to −59 cal B.P.). This procedure is analogous to calculating the moving window average frequency of fire events, but it provides a more locally weighted estimate and avoids artifacts associated with moving windows with sharp boundaries. The SD of the kernel distribution (i.e., the kernel bandwidth) was chosen to highlight variability over specific timescales. Noting that ∼95% of Gaussian kernel mass falls within a range of ±2 SD, we chose kernels with SD values of 2.5, 25, and 250 y to represent nominally decadal, centennial, and millennial variability, respectively. To obtain a confidence interval for estimated FF, we assumed a Poisson distribution on the number of events observed within a given kernel-defined window, defined exposure time as the total number of record-years spanned by the kernel, and followed calculations derived in epidemiology from the relationship between the Poisson and χ^2 distributions (57).

Estimating Regional Biomass Burning. Recently developed methods provide a useful framework for quantitatively combining charcoal records to estimate regional- to global-scale trends in biomass burning (19, 20). A key step in the method is the normalization of individual CHAR records by Box–Cox transformation. Normalization is useful when the component records follow very dissimilar distributions (e.g., when they represent the fire regimes of multiple biomes) and implicitly required by the classical regression methods used subsequently to develop the composite CHAR record. However, many charcoal records are based on discrete particle counts, such that CHAR values of zero are not uncommon. Zero counts are particularly prevalent in the YF cores because of their high sampling resolution and, in some cases, large proportion of charcoal-poor allochthonous silts. As a result of the large proportion of samples in our records with CHAR = 0 (3.9–50.4% of samples within individual records; 16.7% overall), no transformation of the data produced acceptably normal distributions. We did observe an excellent fit of our nonzero CHAR values to the log-normal distribution, suggesting that we should log-transform the data. However, for data containing zeros, this transformation traditionally requires the addition of a small, arbitrary constant to all values, and we found the choice of this constant unduly influenced our results.

Thus, we developed a method that is analogous to the approach used in ref. 19, but designed to permit zero counts and fit the untransformed data. This method begins with the assumption that CHAR is essentially log-normally distributed but that zero values arise from the discretization of finite count data. In this case, CHAR values within a single record or segment thereof can be expected to fit a zero-inflated log normal (ZIL) (58) distribution defined by the probability density function

$$f(x|\mu,\sigma^2,\varphi)=\begin{cases}(1-\varphi)\dfrac{1}{x\sqrt{2\pi\sigma^2}}e^{-\frac{(\ln(x)-\mu)^2}{2\sigma^2}} & x>0\\ \varphi & x=0\end{cases},$$

where x is a particular CHAR value, φ is the proportion of zeros in the population of CHAR values, and μ and σ^2 are the mean and variance, respectively, of the nonzero CHAR values in the log domain.

To develop a composite CHAR estimate from multiple records, we first standardized each record in the log domain by log-transforming the nonzero CHAR in the record, applying a z-score transformation, and then returning to the linear domain by exponentiation. We then used kernel-weighted local likelihood estimation (59) to obtain the ZIL parameters that provided the best fit to the standardized data in the neighborhood of target estimation points spanning the composite dataset in annual increments. For each target point, we first assigned a weight to every standardized CHAR value using a Gaussian kernel (with SD values of 2.5, 25, or 250 y as described for FF estimation). We then numerically solved for the ZIL parameters that maximized the local likelihood, defined as the kernel-weighted sum of the log likelihoods of all individual data points. Finally, we defined composite CHAR at the target point as the mean of the best fit ZIL distribution, which is given by

$$(1-\theta)\left(e^{\mu+\sigma^2/2}\right).$$

Confidence intervals were derived from parametric bootstrap sampling from the fitted distribution.

Validation of CHAR and FF Composite Records. To evaluate the ability of CHAR and FF composite records to capture fire activity over a range of spatial scales, we compared the records to observational fire data from 1950 to 2008 CE in the Alaska Large Fire Database (12) maintained by the US Bureau of Land Management. We summarized observed area burned within study areas defined by various radii (ranging from 1 to 100 km) around all study sites (Fig. 1). We transformed and smoothed these data analogously to composite CHAR and evaluated the correlation between observed area burned and composite CHAR at each spatial scale (Fig. 2 *A* and *B*). Significance was estimated by block bootstrap resampling (60). There are too few fires in the observational record to estimate regional FF directly (i.e., from the time between consecutive fires at a particular location). Instead, for each spatial scale considered, we determined the proportional area burned within the entire study area (defined by radii around all sites as described above) from 1950 to 2008 CE, and from this quantity, we estimated mean FF using the method described in ref. 33. We then compared these estimates with the mean charcoal-inferred FF for the entire validation period, calculating percent error as the difference between the estimates divided by the observation-based value (Fig. 2*C*).

ACKNOWLEDGMENTS. We thank C. Barrett, J. Beamer, B. Clegg, T. Vuong, C. Walsh, and K. Wolfe for field and laboratory assistance. This research was supported by National Science Foundation (NSF) Grants ARC-0612366 and ARC-1023477 (F.S.H.). R.K. was an NSF GK-12 Fellow and a Dissertation Completion Fellow at the University of Illinois. P.E.H. was a National Parks Ecological Research Fellow.

1. Apps MJ, et al. (1993) Boreal forests and tundra. *Water Air Soil Pollut* 70(1-4):39–53.
2. ACIA (2004) *Impacts of a Warming Arctic: Arctic Climate Impact Assessment* (Cambridge Univ Press, Cambridge, United Kingdom).
3. Kasischke ES, O'Neill KP, French NHF, Bourgeau-Chavez LL (2000) *Fire, Climate Change, and Carbon Cycling in the Boreal Forest*, eds Kasischke ES, Stocks BJ (Springer, New York), pp 173–196.
4. Bond-Lamberty B, Peckham SD, Ahl DE, Gower ST (2007) Fire as the dominant driver of central Canadian boreal forest carbon balance. *Nature* 450(7166):89–92.
5. Randerson JT, et al. (2006) The impact of boreal forest fire on climate warming. *Science* 314(5802):1130–1132.
6. Liu H, Randerson JT, Lindfors J, Chapin FS III (2005) Changes in the surface energy budget after fire in boreal ecosystems of interior Alaska: An annual perspective. *J Geophys Res* 110:D13101.
7. Duffy PA, Walsh JE, Graham JM, Mann DH, Rupp TS (2005) Impacts of large-scale atmospheric-ocean variability on Alaskan fire season severity. *Ecol Appl* 15(4):1317–1330.
8. Balshi M, et al. (2009) Assessing the response of area burned to changing climate in western boreal North America using a Multivariate Adaptive Regression Splines (MARS) approach. *Glob Chang Biol* 15(3):578–600.
9. Beck PSA, et al. (2011) The impacts and implications of an intensifying fire regime on Alaskan boreal forest composition and albedo. *Glob Chang Biol* 17(9):2853–2866.
10. Flannigan MD, Krawchuk MA, De Groot WJ, Wotton BM, Gowman LM (2009) Implications of changing climate for global wildland fire. *Int J Wildland Fire* 18(5): 483–507.
11. Johnstone JF, Rupp TS, Olson MA, Verbyla DL (2011) Modeling the impacts of fire severity on successional trajectories and future fire behavior in Alaskan boreal forests. *Landsc Ecol* 26(4):487–500.
12. Kasischke ES, Williams D, Barry D (2002) Analysis of the patterns of large fires in the boreal forest region of Alaska. *Int J Wildland Fire* 11(2):131–144.
13. Stocks BJ, et al. (2002) Large forest fires in Canada, 1959–1997. *J Geophys Res* 108, 10.1029/2001JD000484.
14. Gavin DG, et al. (2007) Forest fire and climate change in western North America: Insights from sediment charcoal records. *Front Ecol Environ* 5:499–506.
15. Marlon JR, et al. (2009) Wildfire responses to abrupt climate change in North America. *Proc Natl Acad Sci USA* 106(8):2519–2524.
16. Higuera PE, Peters ME, Brubaker LB, Gavin DG (2007) Understanding the origin and analysis of sediment-charcoal records with a simulation model. *Quat Sci Rev* 26(13):1790–1809.
17. Higuera PE, Whitlock C, Gage JA (2011) Linking tree-ring and sediment-charcoal records to reconstruct fire occurrence and area burned in subalpine forests of Yellowstone National Park, USA. *Holocene* 21(2):327–341.
18. Ali AA, et al. (2012) Control of the multimillennial wildfire size in boreal North America by spring climatic conditions. *Proc Natl Acad Sci USA* 109(51):20966–20970.
19. Marlon JR, et al. (2008) Climate and human influences on global biomass burning over the past two millennia. *Nat Geosci* 1(10):697–702.
20. Marlon JR, et al. (2012) Long-term perspective on wildfires in the western USA. *Proc Natl Acad Sci USA* 109(9):E535–E543.
21. Kelly R, Higuera PE, Barrett CM, Hu FS (2011) A signal-to-noise index to quantify the potential for peak detection in sediment–charcoal records. *Quat Res* 75(1):11–17.
22. Hu FS, et al. (2006) How climate and vegetation influence the fire regime of the Alaskan boreal biome: The Holocene perspective. *Mitig Adapt Strategies Glob Change* 11(4):829–846.
23. Higuera PE, Brubaker LB, Anderson PM, Hu FS, Brown TA (2009) Vegetation mediated the impacts of postglacial climate change on fire regimes in the south-central Brooks Range, Alaska. *Ecol Monogr* 79(2):201–219.
24. Viereck LA, Cleve KV, Dyrness CT (1986) *Forest Ecosystems in the Alaskan Taiga*, eds Cleve KV, Chapin FS, Flanagan PW, Viereck LA, Dyrness CT, III (Springer, New York), pp 22–43.
25. Clegg BF, Kelly R, Clarke GH, Walker IR, Hu FS (2011) Nonlinear response of summer temperature to Holocene insolation forcing in Alaska. *Proc Natl Acad Sci USA* 108(48): 19299–19304.
26. Tinner W, et al. (2008) A 700-year paleoecological record of boreal ecosystem responses to climatic variation from Alaska. *Ecology* 89(3):729–743.
27. Diaz HF, et al. (2011) Spatial and temporal characteristics of climate in Medieval Times revisited. *Bull Am Meteorol Soc* 92:1487.
28. Hu FS, Ito E, Brown TA, Curry BB, Engstrom DR (2001) Pronounced climatic variations in Alaska during the last two millennia. *Proc Natl Acad Sci USA* 98(19):10552–10556.
29. Clegg BF, Hu FS (2010) An oxygen-isotope record of Holocene climate change in the south-central Brooks Range, Alaska. *Quat Sci Rev* 29(7-8):928–939.
30. Mann DH, Heiser PA, Finney BP (2002) Holocene history of the Great Kobuk sand dunes, northwestern Alaska. *Quat Sci Rev* 21(4):709–731.
31. Hinzman LD, et al. (2005) Evidence and implications of recent climate change in northern Alaska and other Arctic regions. *Clim Change* 72(3):251–298.
32. Kasischke ES, et al. (2010) Alaska's changing fire regime—implications for the vulnerability of its boreal forests. *Can J Res* 40(7):1313–1324.
33. Johnson EA, Gutsell SL (1994) *Advances in Ecological Research*, eds Begon M, Fitter AH (Academic, London), pp 239–287.
34. Viereck LA (1973) Wildfire in the taiga of Alaska. *Quat Res* 3(3):465–495.
35. Johnstone JF, Chapin FS III (2006) Effects of soil burn severity on post-fire tree recruitment in boreal forest. *Ecosystems* 9(1):14–31.
36. Johnstone JF, et al. (2010) Fire, climate change, and forest resilience in interior Alaska. *Can J Res* 40(7):1302–1312.
37. Booth RK, et al. (2012) Multi-decadal drought and amplified moisture variability drove rapid forest community change in a humid region. *Ecology* 93(2):219–226.
38. Mann DH, Rupp TS, Olson MA, Duffy PA (2012) Is Alaska's boreal forest now crossing a major ecological threshold? *Arct Antarct Alp Res* 44(3):319–331.
39. Chapin FS, 3rd, et al. (2005) Role of land-surface changes in arctic summer warming. *Science* 310(5748):657–660.
40. Schuur EAG, Abbott B (2011) Climate change: High risk of permafrost thaw. *Nature* 480(7375):32–33.
41. Osterkamp TE, et al. (2000) Observations of thermokarst and its impact on boreal forests in Alaska, USA. *Arct Antarct Alp Res* 32(3):303–315.
42. Lloyd AH (2005) Ecological histories from Alaskan tree lines provide insight into future change. *Ecology* 86(7):1687–1695.
43. Myers-Smith IH, et al. (2011) Shrub expansion in tundra ecosystems: Dynamics, impacts and research priorities. *Environ Res Lett* 6(4):045509.
44. Hu FS, et al. (2010) Tundra burning in Alaska: Linkages to climatic change and sea ice retreat. *J Geophys Res* 115, 10.1029/2009JG001270.
45. Serreze MC, Holland MM, Stroeve J (2007) Perspectives on the Arctic's shrinking sea-ice cover. *Science* 315(5818):1533–1536.
46. Turetsky MR, et al. (2010) Recent acceleration of biomass burning and carbon losses in Alaskan forests and peatlands. *Nat Geosci* 4(1):27–31.
47. NALC (2005) *2005 North American Land Cover at 250 m Spatial Resolution* [Natural Resources Canada/Canadian Center for Remote Sensing (NRCan/CCRS), United States Geological Survey (USGS); Insituto Nacional de Estadística y Geografía (INEGI), Comisión Nacional para el Conocimiento y Uso de la Biodiversidad (CONABIO) and Comisión Nacional Forestal (CONAFOR, Montreal)].
48. Johnstone JF, Hollingsworth TN, Chapin FS III, Mack MC (2010) Changes in fire regime break the legacy lock on successional trajectories in Alaskan boreal forest. *Glob Chang Biol* 16(4):1281–1295.
49. Flannigan MD, Stocks BJ, Turetsky MR, Wotton M (2009) Impacts of climate change on fire activity and fire management in the circumboreal forest. *Glob Chang Biol* 15(3):549–560.
50. McGuire AD, Chapin FS III, Walsh JE, Wirth C (2006) Integrated regional changes in Arctic climate feedbacks: Implications for the global climate system. *Annu Rev Environ Resour* 31:61–91.
51. Gallant AL, Binnian EF, Omernik JM, Shasby MB (1995) *Ecoregions of Alaska* (US Government Printing Office, Washington, DC).
52. Binford MW (1990) Calculation and uncertainty analysis of 210Pb dates for PIRLA project lake sediment cores. *J Paleolimnol* 3(3):253–267.
53. Oswald WW, et al. (2005) Effects of sample mass and macrofossil type on radiocarbon dating of arctic and boreal lake sediments. *Holocene* 15(5):758–767.
54. Stuiver M, Reimer PJ (1993) Extended 14C data base and revised CALIB 3.0 14C age calibration program. *Radiocarbon* 35(1):215–230.
55. Colombaroli D, Gavin DG (2010) Highly episodic fire and erosion regime over the past 2,000 y in the Siskiyou Mountains, Oregon. *Proc Natl Acad Sci USA* 107(44): 18909–18914.
56. Faegri K, Iversen J (1989) *Textbook of Pollen Analysis* (Wiley, New York).
57. Ulm K (1990) A simple method to calculate the confidence interval of a standardized mortality ratio (SMR). *Am J Epidemiol* 131(2):373–375.
58. Aitchison J (1955) On the distribution of a positive random variable having a discrete probability mass at the origin. *J Am Stat Assoc* 50(271):901–908.
59. Staniswalis JG (1989) The kernel estimate of a regression function in likelihood-based models. *J Am Stat Assoc* 84(405):276–283.
60. Gavin DG, et al. (2011) Abrupt Holocene climate change and potential response to solar forcing in western Canada. *Quat Sci Rev* 30(9-10):1243–1255.